AIRCRAFT/LIDAR TURBULENCE COMPARISON

Kao-Huah Huang
FWG Associates, Inc.

Introduction

A field test was carried out to compare lidar-measured winds and turbulence with both aircraft measurements and tower array measurements. The instrumentation consisted of the NASA/MSFC (NASA/Marshall Space Flight Center) lidar (Bilbro and Vaughan 1978), the NASA B-57B instrumented aircraft (Campbell et al. 1983), and the NASA/MSFC Atmospheric Boundary Layer Facility eight-tower array (Frost and Lin 1983). The experiment called for flights on May 10, 11, and 12, 1983. The May 12 experiment is reported here. Details on the other flights are given in Frost and Huang (1983).

On May 12, 1983, the lidar was fixed at a 6^{o} vertical angle and at 52^{o} azimuthal from true north, see Figure 1. The aircraft then flew approach paths at an approximate 4^{o} glide slope parallel to the radar beam. Eight successive runs or approach paths were flown at approximately 5-minute intervals.

The emphasis of the study was to compare Doppler lidar-measured winds and turbulence with aircraft measurements. Primarily the study was to compare aircraft-measured turbulence intensities with the lidar second moment or spectral width data. Unfortunately, this aspect of the study was not particularly successful in view of the fact that only three range bins (Range Bins 9, 10, and 11) had high enough signal-to-noise ratios for the second moments to be successfully computed. Secondly, the values were computed in the range from 1.26 to 2.51 m/s, which is a factor of ten larger than those values measured either with the aircraft or with the tower array.

The field study was successful, however, in that it: 1) provided a unique set of data for comparing mean wind speed values; 2) revealed that turbulence intensities computed from the Doppler-measured wind speed time histories (i.e., 300 m spatially averaged values) agree remarkably well with the point measurement from the aircraft; and 3) showed that turbulence spectra calculated both from the time histories of the lidar-measured winds, and the aircraft-measured winds, were in very good agreement.

Finally, an extremely interesting atmospheric boundary-layer event evolved during the time period (16:42–17:28 Z) of the May 12 test. This event was clearly recorded by both the aircraft instrumentation and the lidar. Because both systems accurately recorded this boundary-layer event, it is believed that considerable

reliability in the lidar mean winds is demonstrated.

This report presents a detailed analysis of the winds measured during the evolution of the atmospheric boundary layer occurring on May 12 and emphasizes the validation of the Doppler lidar remote measurements with the in situ aircraft measurements.

Instrumentation and Data

A complete description of the NASA/MSFC Doppler lidar is provided in Bilbro and Vaughan (1978), Jeffreys and Bilbro (1975), and Lee (1982). The lidar is a variably pulsed CO_2 Doppler lidar. During this study, a 2-μs-pulsed lidar was used. The Doppler measures the component of the wind along the lidar beam, i.e., the radial wind speed component. The measurements are representative of the average wind speed within a conical trapezoid of 300 m in length and of diameter associated with the diverging lidar beam width. Figure 1 illustrates the lidar beam and shows the location of each individual range bin for which radial wind speed components are measured. The figure also illustrates the position of the beam relative to the terrain contour cross section.

The lidar data were received from NASA/MSFC in digitized format on magnetic tapes. Typical time histories of the data provided on the tape, which includes amplitude of the signal in decibels, radial wind velocity in meters per second (m/s), and second moment (lidar width) data for turbulence intensities in meters per second, are shown in Figure 2 for the May 10 and 12 field tests, respectively.

Figure 3 is a plot of 150 sequential values of wind velocity from the May 12 data tape. The figure illustrates approximately 75 seconds of data. It is clear from the figure that data in Range Bins 1 through 8 are very noisy due to ground clutter and do not provide useful data. Also, the figure shows that beyond approximately Range Bin 21, the signal-to-noise ratio becomes excessive and velocities measured above this altitude are not meaningful. Thus, for the May 12 field test, only radial wind speed values from Range Bin 9 (460 m msl) to Range Bin 21 (840 m msl) were selected for analysis.

Data from the B-57B flights consisted of 80 variables in a 60-bit integer format. The original raw data were sampled at 200 cycles per second. However, they were provided from NASA Langley Research Center in engineering units at 40 samples per second. Although all the variables necessary to resolve the wind speed components by backing out the aircraft motion are available, the data from NASA Langley provided pre-computed gust velocities. These were used throughout the analysis.

Figure 1 shows typical flight paths relative to the lidar beam. Because of un-

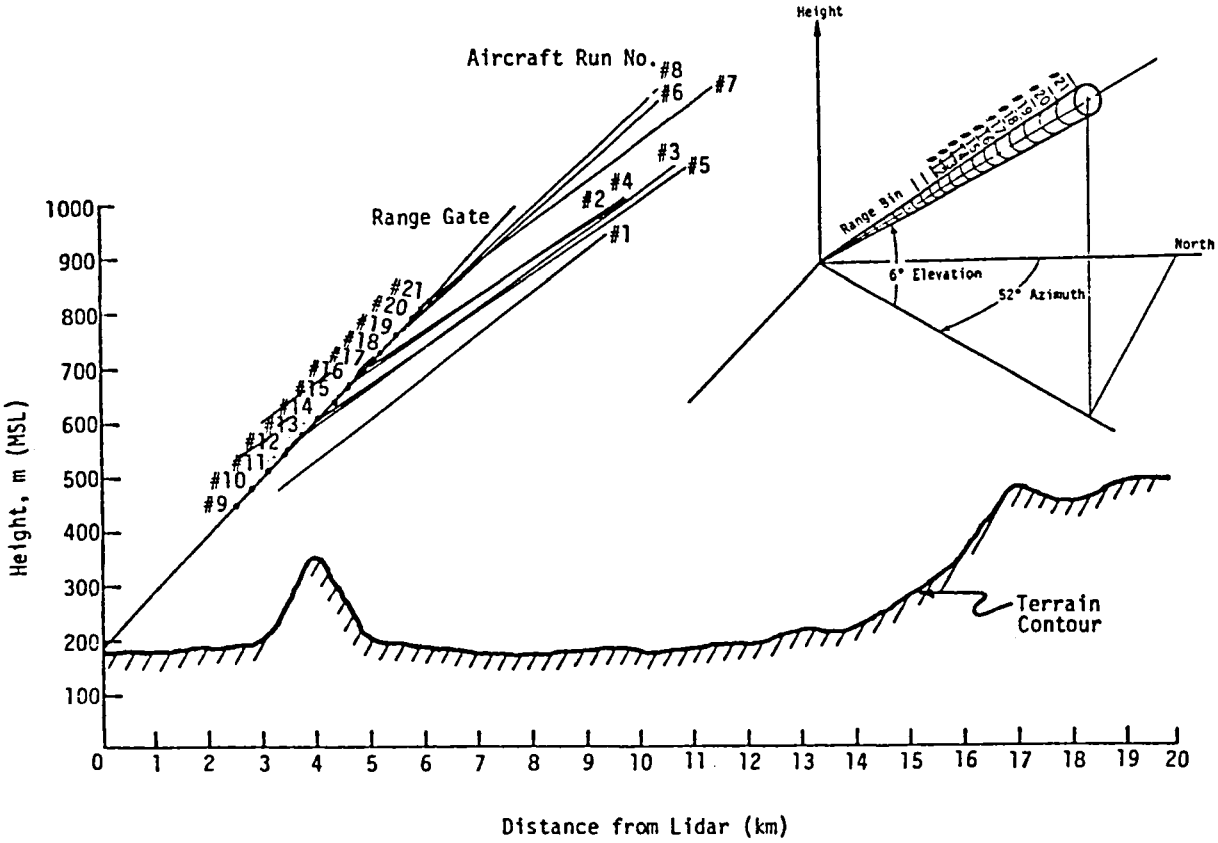

Figure 1. Lidar beam range bins at 6^{0} vertical and 52^{0} azimuth and relative positions of aircraft flight paths.

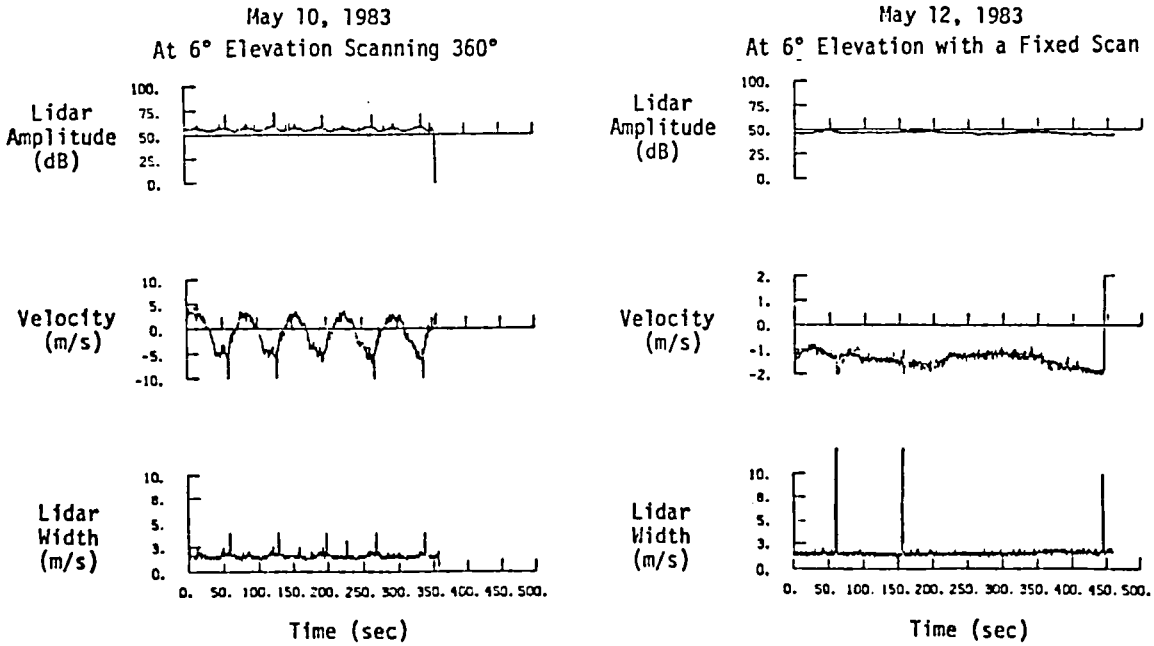

Figure 2. Typical time series of lidar amplitude, velocity, and spectrum width for Range Bin 9.

usual drift in the INS, the latitude and longitude measurements are questionable. Thus the exact position of the aircraft relative to the lidar beam in a horizontal plane is not know precisely. Ground-based personnel, however, observed the aircraft to approach essentially along the position of the lidar beam. The aircraft height, however, at any instant is accurately measured and is, in fact, the most important value of aircraft position for comparing the wind speeds measured by the two systems.

Figure 4 is a three-dimensional plot of the horizontal winds measured with the aircraft along each flight path and staggered in time. In this plot the wind vectors illustrated are values averaged over a 300 m section along the flight path. One observes the growth of the inversion layer, which was developing at approximately 600 m above the ground, over the 30-minute period during which the eight flights were carried out.

Comparison of Lidar Measurements with Aircraft Measurements

Comparison of the measurements of mean wind with the lidar and with the aircraft system is described in this section. The aircraft-measured wind speeds were first transformed to the time-dependent components along a 6^o line of sight and at 52^o azimuthal true north, i.e., along the lidar beam.

The aircraft-measured wind speeds were then averaged with time over a period corresponding to the length of time required for the aircraft to traverse the 300-m range bins along the flight path. Two approaches to carrying out this averaging technique were investigated. One was to assume vertical homogeneity in the flow field. The averaging process for the aircraft data was then carried out as illustrated in Figure 5a. The alternate technique was to average the wind assuming homogeneity in the horizontal direction. This approach is illustrated in Figure 5b.

A third effect taken into account when comparing data from the two systems was to assure that the winds measured with lidar and with the aircraft were measured in the same time period. The run times associated with each flight path were, therefore, overlaid on the lidar-measured winds as illustrated in Figure 6. The lidar data are sampled in each bin at approximately 0.5-second intervals. The segment of the lidar wind speed time history associated with the time period in which the aircraft was passing through or parallel to that range bin was then averaged.

Figure 7 compares the lidar-measured winds averaged over the time period, as described above, with the aircraft-measured winds averaged over the corresponding 300-m section assuming vertical homogeneity. Horizontal homogeneity showed similar results. One observes very good agreement between the lidar measurements and aircraft measurements although the data are consistently higher for the lidar

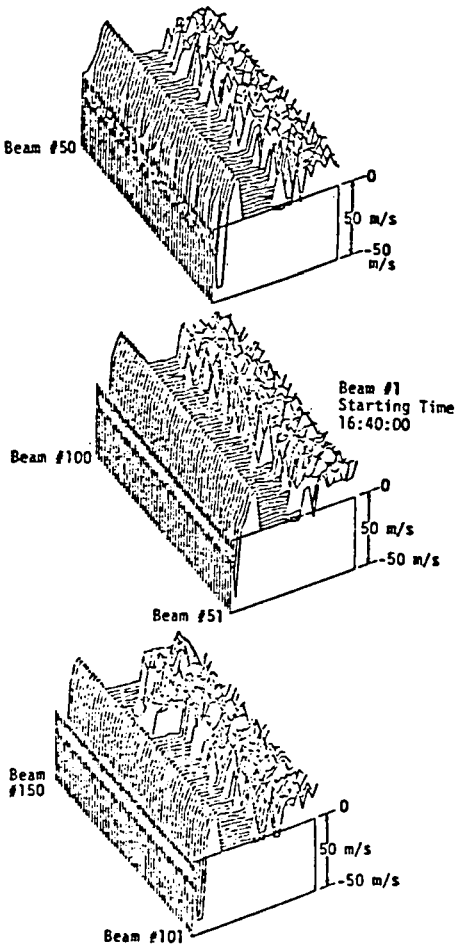

Figure 3. Sample of velocity data along the lidar beam for 150 sequential beams (represents 75 seconds of data).

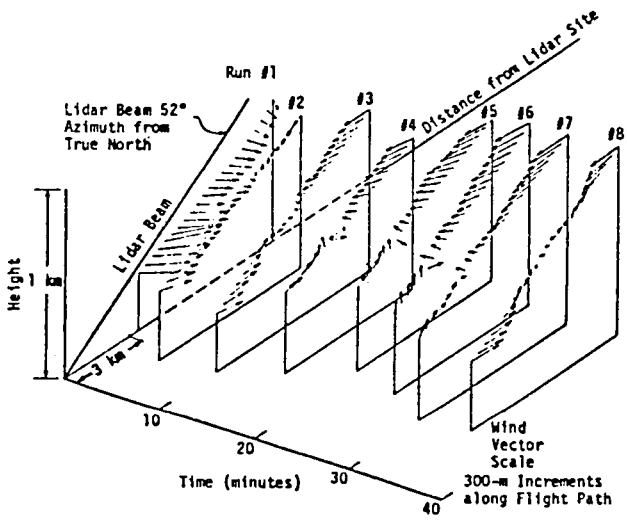

Figure 4. Horizontal wind vectors along B-57B flight path (May 12, 1983).

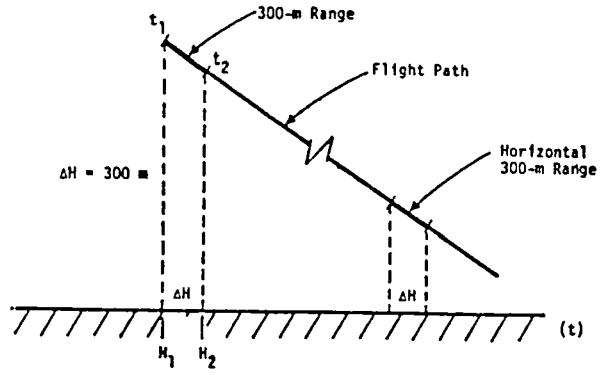

(a)

$$\bar{W} = \frac{1}{(N_2 - N_1 + 1)} \sum_{i=N_1}^{N_2} w_i$$

$$N_1 = \frac{t_1 - t_0}{0.025} \qquad N_2 = \frac{t_2 - t_0}{0.025}$$

t_0 = beginning of each run

t_1 = time airplane enters each horizontal range at H_1

t_2 = time airplane leaves each horizontal range at H_2

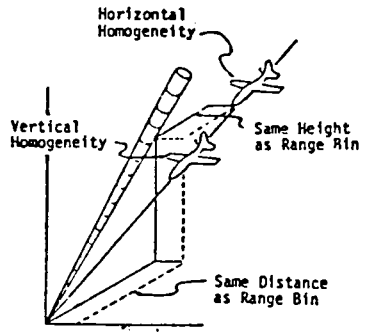

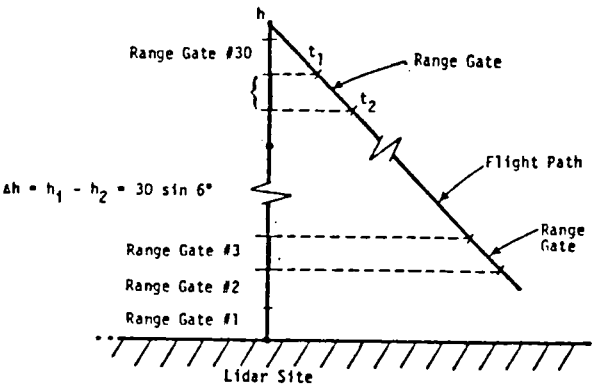

(b)

$$\bar{W} = \frac{1}{(N_2 - N_1 + 1)} \sum_{i=N_1}^{N_2} w_i$$

$$N_1 = \frac{t_1 - t_0}{0.025} \qquad N_2 = \frac{t_2 - t_0}{0.025}$$

t_0 = beginning of each run

t_1 = time airplane enters each range gate at height h_1

t_2 = time airplane leaves each range gate at height h_2

Figure 5. Evaluation procedure for averaging B-57B wind for each range bin.

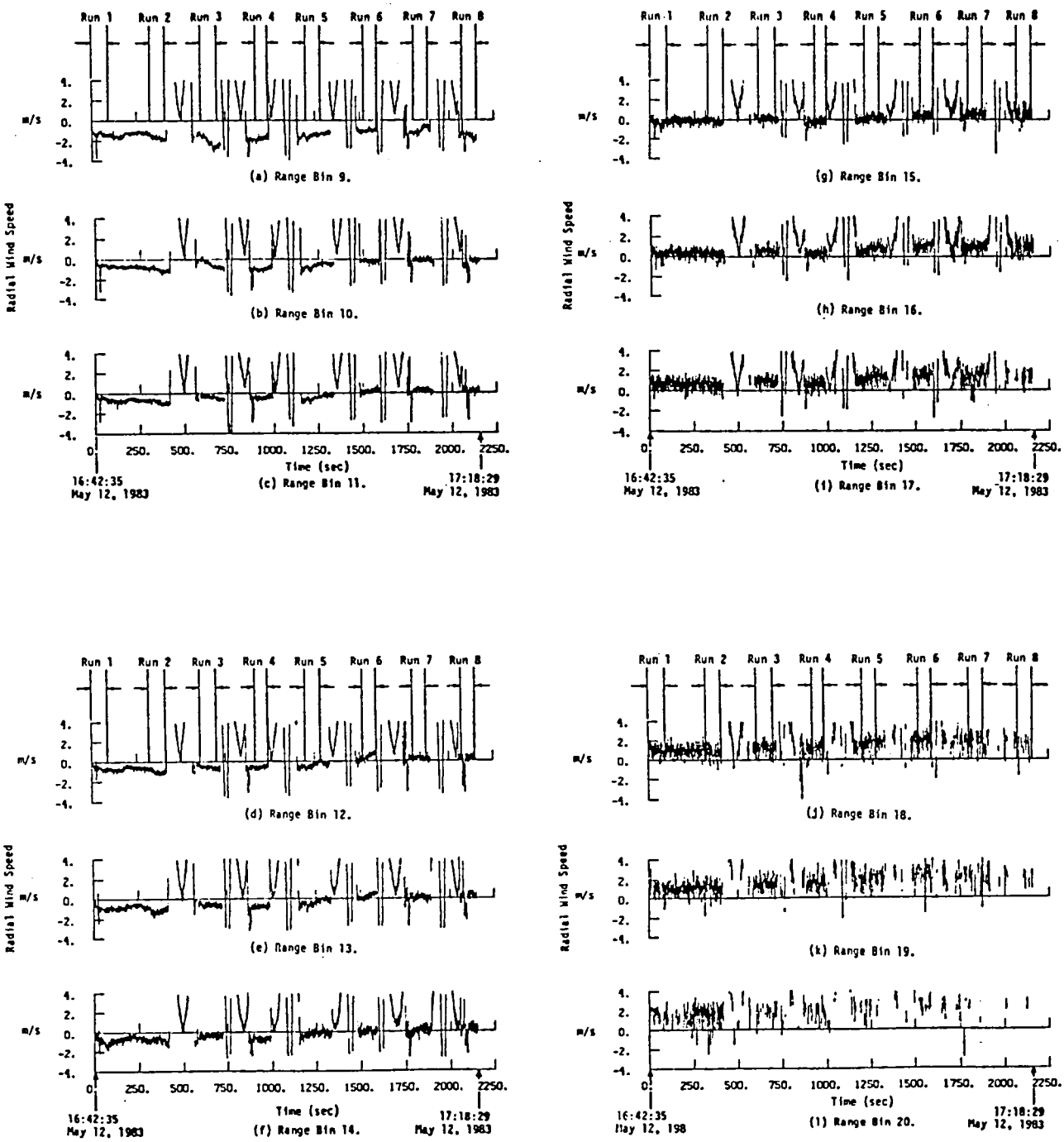

Figure 6. Time histories of radial wind velocity from lidar measurements.

measurements. Although the exact cause of this difference is not known, it is reasonable to assume that due to the unusual drift in the INS the aircraft velocity may be low because of the Schuler oscillation phenomenon.

In general, the trends of the aircraft-measured wind most closely follow the lidar measurements when the assumption of vertical homogeneity is made. This implies that the best agreement is achieved when the aircraft is at the same distance from the lidar even though it may be above or below the lidar beam at that distance. Horizontal homogeneity, of course, implies that the aircraft is making measurements at the same height as the lidar beam for the given range bin, but may be further from, or closer to, the lidar location in horizontal distance. It should be noted that no attempt is made to correct the velocities for convective effects, i.e., translation of the air parcel parallel to the lidar beam, nor for surface terrain contour effects. A terrain correction may help improve the data comparison since the lidar beam passed directly over the top of a mountain, whereas some of the flight paths may have passed to one side or the other. The agreement of the data is believed to be sufficiently good that no terrain correction was attempted.

Computed turbulence intensities for the radial wind speed component from the aircraft measurements and the lidar measurements are also shown in Figure 7. In the figure, the turbulence intensity of the lidar-measured wind is computed from:

$$\sigma_w = \frac{1}{N}\sqrt{\sum_{n=1}^{N}(W(t) - \bar{W})^2} \tag{1}$$

where $\bar{W}$ is the average wind speed for the period of time the aircraft passes through or parallel to the range bin of interest and $W(t)$ is the fluctuation in wind. The summation is carried out over N time increments of $\Delta t = 0.455$ second which lapses the time interval between the aircraft entering and leaving the range bin. This time interval is used both in computing the aircraft turbulence intensity, illustrated in the figure by the small plus signs, and the lidar turbulence intensity, indicated by the small circles. The interesting result is that the turbulence intensities, although scattered, are intermingled, indicating general agreement between the lidar-measured turbulence intensity and the aircraft-measured values. This is particularly true for the lower range bins.

This result is an important observation. It is apparent that results from the present study contradict this thinking. It is generally thought that the Doppler second moment data will correlate with essentially point measured turbulence intensities obtained from the aircraft. The fluctuations in the radial wind component time history, on the other hand, being values of wind averaged over the spatial

extent of the range bin, are thought to not necessarily correspond to turbulence measured internal to the volume element.

As noted earlier, only three range bin values of spectral width determined turbulence intensities could be extracted from the lidar signal. These values range from 1.26 to 2.51 m/s; almost a factor of ten larger than values measured by the aircraft or computed from the lidar data as described above.

In order to investigate the turbulence measurements further, the turbulent energy spectra were computed. Turbulence spectra was computed for each of the eight flight paths and at each corresponding range bin, assuming vertical homogeneity. The spectrum computed for each range bin for the eight aircraft flights was then segment averaged to provide the spectra illustrated by the small plus signs in Figure 8. Similarly, spectra for a 2-minute time period begin at the time the aircraft enters the range bin, or a region parallel to it, were then computed from the lidar data. Note these data are sampled at approximately two times per second resulting in a Nyquist frequency of approximately 1 Hz. The aircraft data, on the other hand, are sampled at 40 times per second resulting in a Nyquist frequency of 20 Hz. The spectra computed from the lidar data were only five segment averaged. The reason for this is illustrated by inspection of Figure 6. At times, corresponding to some of the later aircraft flights, the radial wind measured by the lidar at the higher elevations or higher numbered range bins (i.e., approximately Range Bins 16 through 21) was extremely intermittent. This is probably due to cloud formation during the later runs. Therefore, although these time histories provide a reasonably valid average or mean wind speed, they do not allow a valid spectrum to be computed. At the lower range bins (i.e., Range Bins 11 through 16), very good agreement with the aircraft data is observed. Note Range Bins 9 and 10 were not used because very few aircraft flights descend to that height.

Although the data do not fall on top of one another because of the different sampling frequencies involved, the spectra do merge together forming a relatively continuous line. This indicated that the distribution of turbulent intensity in the frequency domain is essentially the same for both measurements. The disagreement in spectra at the higher range bins is due to increasing noise or decreasing signal-to-noise ratio, which is clearly apparent in Figure 6.

The very good agreement both in turbulence intensity, and in turbulence spectral properties occurring in the clear-air measurements, leads to the conclusion that computed values of turbulence properties using the time history of the lidar-measured winds provide highly meaningful results. Although further research is required, this suggests that the second moment or spectral width of the Doppler frequency from the lidar may not be necessary in order to compute turbulence properties. If this is true, the time history of the wind speeds measured by the lidar can

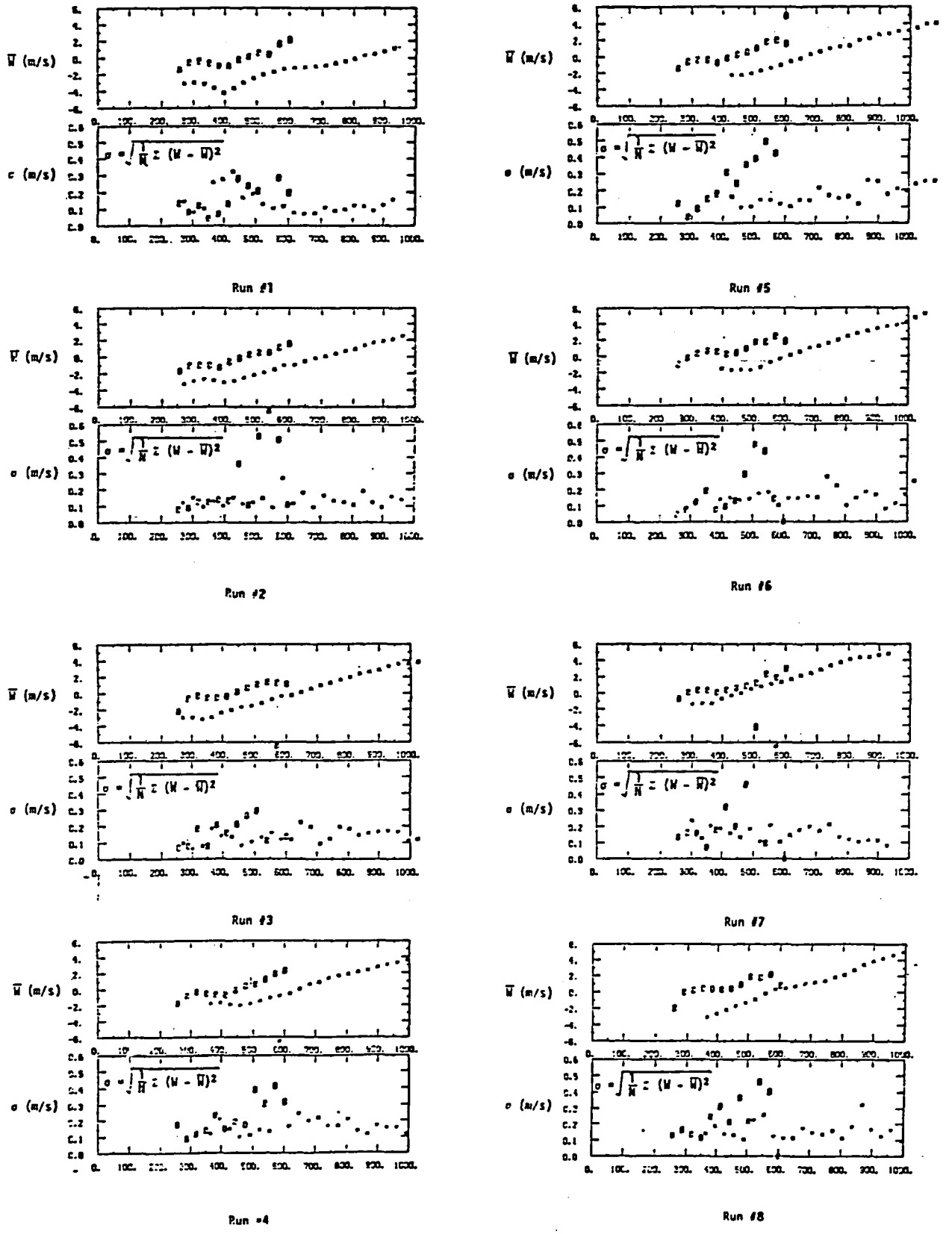

Figure 7. Comparison of lidar-measured winds with aircraft-measured winds and computed turbulence (assumed vertical homogeneity); Aircraft = x, Lidar = Ø.

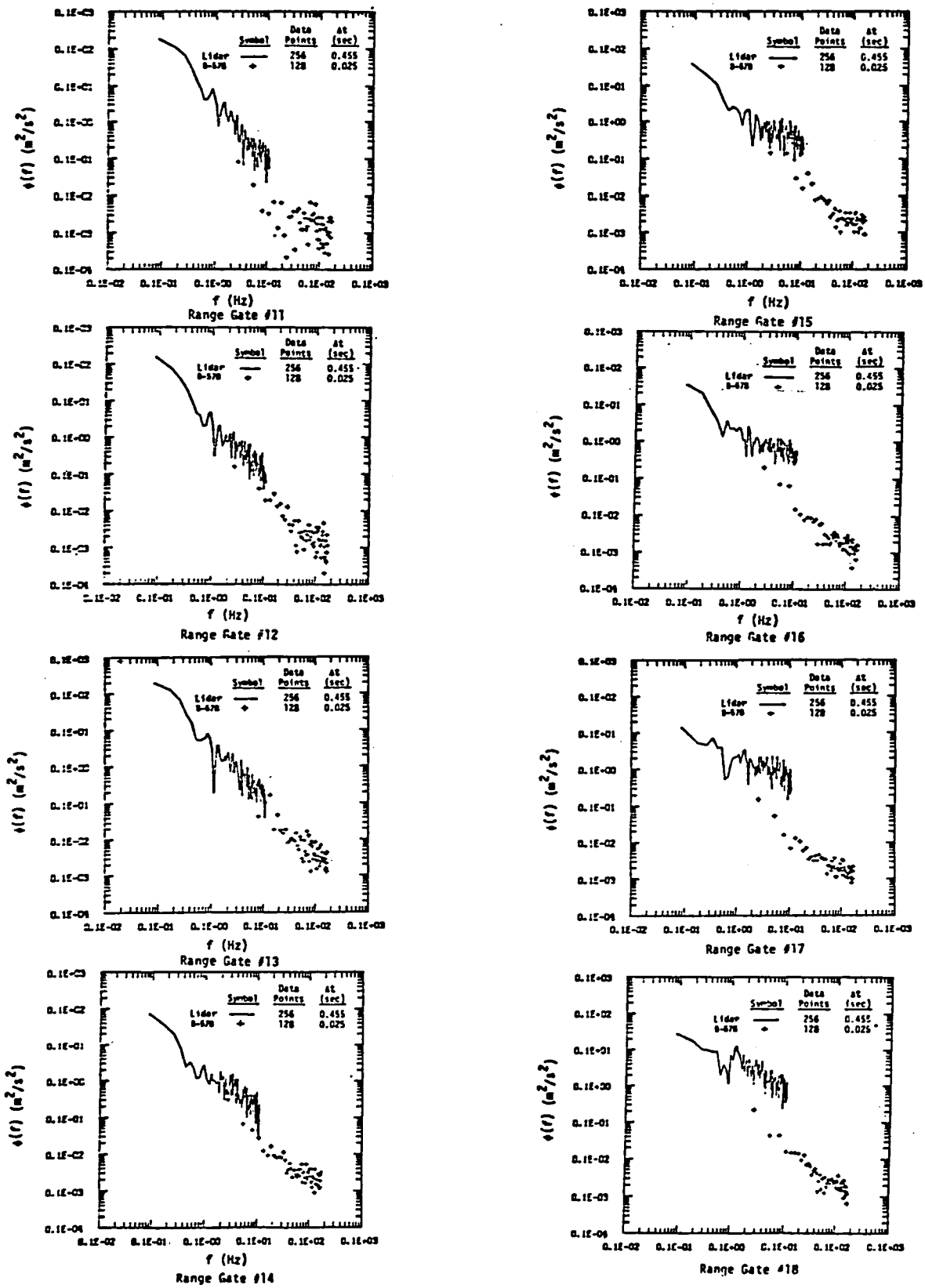

Figure 8. Radial velocity spectra.

simply be analyzed for turbulent statistical properties of interest.

Conclusions

It is concluded that very good agreement between remotely sensed winds using a ground-based Doppler lidar and in situ measurements with an instrumented aircraft is possible. Results show that turbulence intensities computed from time histories measured with the aircraft and time histories of the radial wind measured with lidar can be analyzed statistically to provide turbulence intensities and turbulence spectra which agree well with one another. The results further show that the second moment data, as presently compared with the NASA/MSFC algorithms, do not provide meaningful comparisons with turbulence intensities measured with the aircraft. This disagreement, however, must be investigated further in terms of the accuracy of the second moment data determined by both the lidar hardware and the algorithm for computing the second moment.

References

Bilbro, J. W. and W. W. Vaughan (1978): "Wind Field Measurement in the Nonprecipitous Regions Surrounding Severe Storms by an Airborne Pulsed Doppler Lidar System," Bulletin of the Am. Met. Soc., 59(9): 1095.

Campbell, W., D. W. Camp, W. Frost (1983): "An Analysis of Spanwise Gust Gradient Data," Preprints: Ninth Conference on Aerospace and Aeronautical Meteorology, June 6-9, 1983, Omaha, NE, Am. Met. Soc., Boston, MA.

Frost, W. and K. H. Huang (1983): "Doppler Lidar Signal and Turbulence Study," Final report prepared for NASA Marshall Space Flight Center under Contract NAS8-35185 by FWG Associates, Inc., Tullahoma, TN.

Frost, W and M. C. Lin (1983): "Statistical Analysis of Turbulence Data from the NASA Marshall Space Flight Center Atmospheric Boundary Layer Tower Array Facility," NASA CR 3737.

Jeffreys, H. B. and J. W. Bilbro (1975): "Development of a Laser Doppler System for the Detection and Monitoring of Atmospheric Disturbances," NASA TM X-64981.

Lee, R. W. (1982): "NASA Airborne Doppler Lidar Program: Data Characteristics of 1981 Wind Field Measurements," Technical Report #1, Prepared for NASA/MSFC under Contract NAS8-34768 by Lassen Research, Manton, CA 96059.